Available online at www.sciencedirect.com
SCIENCE DIRECT®

Journal of the European Ceramic Society 23 (2003) 2769–2775

www.elsevier.com/locate/jeurceramsoc

Dissipation and moving contact lines on non-rigid substrates

M. Voué[a,*], R. Rioboo[a], C. Bauthier[b], J. Conti[b], M. Charlot[b], J. De Coninck[b]

[a]*Centre de Recherche en Modelisation Moleculaire, Materia Nova ASBL, Avenue Copernic, 1, B-7000 Mons, Belgium*
[b]*Centre de Recherche en Modelisation Moleculaire, Universite de Mons-Hainaut, Place du Parc, 20, B-7000 Mons, Belgium*

Abstract

We consider the dynamics of spreading of silicon oil droplets on elastomer thin films, and the associated relaxation of the advancing contact angle. Although the viscoelastic breaking of the droplet is observed on bulk elastomers, according to the studies of Shanahan and coworkers [*C. R. Acad. Sci. Paris* 317 (1993) 1153], we show that the breaking progressively disappears as the elastomer film thins.

Keywords: Films; Interfaces; Mechanical properties; Wettability partial; Wetting

1. Introduction

Except the temperature itself at which are carried out most of the experiments in wettability of metals and ceramics surfaces by liquid metals, one of the most important differences between room and high temperature wetting stays in the deformability of the solid substrate which has to be considered during the dissipation of energy associated to the spreading process (see e.g. Saiz and coworkers' studies[1] and the references therein). At high temperature, a ridge may form under given experimental conditions while wetting experiments carried out at room temperature, i.e. on silicon wafers supporting self assembled organic monolayers (SAMs), assume the non-deformability of the substrate. Softer surfaces, and in particular elastomer surfaces, are therefore interesting models to drawn analogies and try to transfer concepts between high and room temperature spreading experiments, in the absence of chemical reactive phenomena.[2]

The wettability of such softer surfaces has been intensively studied since the mid 1980s by Shanahan and coworkers.[3–6] They showed that the spreading of a liquid droplet at the surface of an elastomer was slowed down due to the propagation of the deformation of the solid surface at the triple line along the sample surface.[3–6] This phenomenon is usually referred to as the "viscoelastic breaking" (Fig. 1). Shanahan and Carré[6] showed that the dynamics of spreading of a liquid droplet on an elastomer surface satisfied the following equation

$$\log[\cos\theta_0 - \cos\theta] \simeq n\log U + \log\left[\frac{\gamma}{2\pi G\epsilon U_0^n}\right] \quad (1)$$

where θ and θ_0 are, respectively, the dynamic (advancing) and the equilibrium contact angle, U is the speed of the contact line, γ the liquid surface tension, G is the elastic shear stress modulus of the material and ε is a cut-off distance for the elastic behavior of the material. U_0 is a characteristic speed defined in such a way that $\Delta = (U/U_0)^n$ is the strain energy dissipated during the ridge motion. n is the exponent characteristics of the viscoelastic breaking. Its theoretical value is $n \simeq 0.60$. Experimental investigations lead, for example, to values of $n = 0.56$ for the spreading of tricresylphosphate (TCP) on two-component silicone rubbers (RTV 630 or RTV 615, General Electric Co.), independently of the liquid viscosity.[6,7]

The deformation of the substrate acts as an additional dissipation channel for the energy during the relaxation process of the advancing contact angle θ towards its equilibrium value θ_0. De Coninck and coworkers[8] considered two sources of energy dissipation during the spreading: the rearrangement of the molecules inside the core of the droplet (i.e. the viscous dissipation) and the hoping of the liquid molecules at the triple line

* Corresponding author. Tel.: +32-65-373-885; fax: +32-65-373-881.
E-mail address: michel.voue@umh.ac.be (M. Voué).
URL: http://galileo.umh.ac.be.

0955-2219/03/$ - see front matter © 2003 Elsevier Ltd. All rights reserved.
doi:10.1016/S0955-2219(03)00288-7

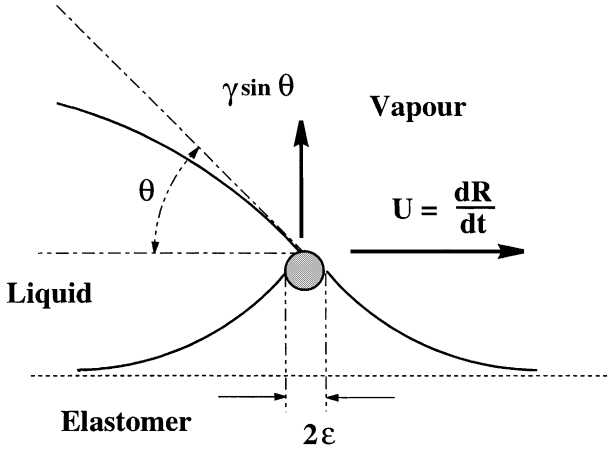

Fig. 1. Spreading of a liquid droplet on a deformable substrate. U is the speed of the contact line, $\gamma\sin\theta$ the force causing the deformation of the elastomer, with θ the advancing contact angle and γ the liquid surface tension.

(Fig. 2), as given by the molecular-kinetic theory (MKT) of wetting.[9,10] Although not considering explicitely the deformation of the substrate, this approach lead to a new formulation of the dynamics of spreading given by:

$$U = \frac{\gamma[\cos\theta_0 - \cos\theta]}{\zeta_0 + 6\eta\Phi\ln(R/a)} \quad (2)$$

where U, θ and θ_0 have the same meaning as in Eq.(1), a is a cutoff length. E is the geometric function that allows the conversion between the contact angle θ and the base radius R of the droplet, within the spherical cap approximation.[8] η is the dynamic viscosity of the spreading liquid. ζ_0 is the friction coefficient of the liquid molecules on the solid substrate and is defined by

$$\zeta_0 = \frac{1}{K_0\lambda^3} \quad (3)$$

where K_0 is the jump frequency of the liquid molecules at the triple line and λ is the average jump length.[10]

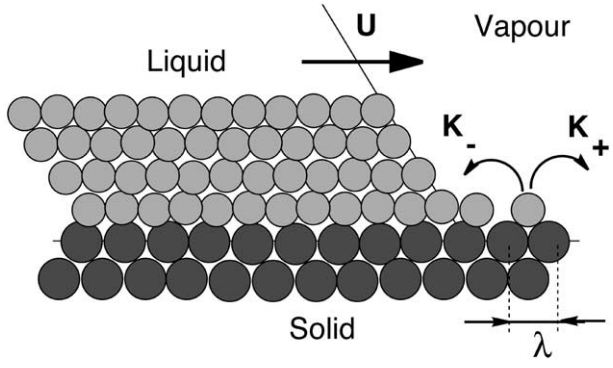

Fig. 2. Displacement of the droplet contact line at speed U according to the molecular-kinetic theory (MKT) of wetting.[9] λ is the average jump length, K_+ and K_- are the jump frequencies in the forward and backward directions. At equilibrium, $K_+ = K_- = K_0$.

The validity of this model has been proved experimentally [11] and numerically,[12] evidencing the existence of several consecutive dissipation regimes (MKT and hydrodynamic regimes) with crossover regimes between them.

In this contribution, we reconsider the spreading of liquid droplets on substrate supported thin elastomer films and investigate the viscoelastic breaking as a function of the film thickness and the impact of water droplets on such surfaces. Experimental techniques and materials are presented in Section 2. Results are given and discussed in Section 3, and conclusions given in Section 4.

2. Materials and experimental techniques

Unless otherwise stated, all the chemical, solvents, ... are analytical grade and were used as purchased, without further purification.

2.1. Substrates preparation

The elastomer substrates and films were made of SI 6600 silicon resin (General Electric), which contains a polydimethylsiloxane (PDMS) mixed with platinum as catalyzer. The PDMS is vinyl-terminated at both ends and has the following physical characteristics: viscosity $\eta = 225$ mPa s at 25 °C, surface tension $\gamma = 22$ mN/m and density $d = 0.97$ g/cm^3. As described in Fig. 3, the elastomer was prepared by mixing the resin and a crosslinker (2.5% w:w).

The crosslinking process occurs by hydrosilylation reaction in the presence of hexane. To obtain the samples referred to as the "bulk elastomer", no extra solvent was added. The mixture is poured in a Petri dish to obtain a 3 mm thick layer and backed in the oven 5 min at 120 °C in a view of obtaining a 100% reticulated elastomer. To obtain glass-supported elastomer films, 0.1 mm thick glass cover slides cleaned using sulfochromic acid were dip-coated in a solution of resin/crosslinker containing from 0 to 33% of hexane. The dipcoating experiments were carried out using a KSV 3000 (KSV Ltd, Finland) setup at a dipping speed of 10 mm per minute. Additionally, an elastomer film supported by a 36 μm-thick polyester (PE) film is prepared

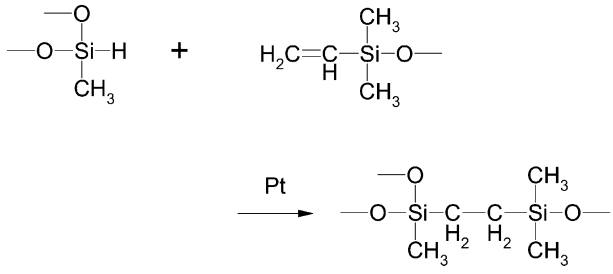

Fig. 3. Crosslinking of vinyl-terminated siloxanes by hydrosilylation reaction.

using a 4 mm diameter bar coater (“RPE-100” sample). The thickness of the films were determined by optical microscopy for the film on PE and by a weighting method for the films on glass (Table 1).

The alkanethiol self-assembled monolayer (SAM) was prepared according to the procedure described by Semal and coworkers.[13] Prior to the deposition of the organic layer, (100) silicon wafers were covered by a 30 Å thick titanium layer and a 500 Å thick gold layer obtained by epitaxial deposition. After degreasing by sonication in chloroform and UV/ozone cleaning, the wafers were immersed for 15 min in ethanol and then for 18 h into the grafting solution at room temperature (≃21 °C). The grafting solution was a 3 mM solution of CH_3–$(CH_2)_{11}$–SH in ethanol. After the reaction, the grafted substrate was rinsed and kept with ethanol for further use.

2.2. Liquids

The liquid used to perform the advancing contact angle relaxation experiments was the resin itself, without crosslinker. When considering the impact of liquid droplets on the elastomer surface and on the alkanethiol SAM, Milli-Q water was used, as described in the next paragraphs.

2.3. High-speed imaging system

High-speed imaging was performed by the use high-speed high-resolution C-MOS motion camera (HCC-1000 by Vosskühler GmbH). High-speed stroboscope and electronic delayer helped to provide images at 923 images per second in this particular case (image resolution: 1024×512 pixels). Contrary to previous work[14–18] where the sequence was reconstructed by mean of repeating experiments, here each sequence is the result of a single drop impact.[19] The liquid used is MilliQ water droplet generated with a step motor syringue pump. Waxed needles allows a high reproducibility in droplet size (diameter drop: 2.340±0.002 mm). The impact velocity was controlled by the height of fall (1.730±0.016 m/s). Both experiments were reproduced several times (at least three times) in order to check the reproducibility of the event.

Table 1
Surface preparation

	Resin / Crosslinker (w:w)	Support	Solvent	Thickness (μm)
$Bulk_1$	39:1	–	–	3000±10
$Bulk_2$	99:1	–	–	3000±10
R-GL0	39:1	Glass cover	–	24.1±1.2
R-GL1	39:1	Glass cover	Hexane 9.1% (v:v)	12.9±0.7
R-GL2	39:1	Glass cover	Hexane 23.0% (v:v)	8.0±0.4
R-GL3	39:1	Glass cover	Hexane 33.0% (v:v)	6.0±0.3
R-PE100	39:1	PE 36 μm-thick	Hexane 50% (w:w)	3.0±0.1

2.4. Relaxation of the advancing contact angle

The static and dynamic contact angles are measured as described in previous articles.[11,13,20] Only an outlook of the experimental procedure is given here. The substrate was placed on a movable stage in front of a microscope and a liquid droplet (volume ≃6 mm^3) was deposited with a syringe. Within a few seconds, the droplet had spread and reached its static contact angle. The viscosity of the liquid was high enough to allow us to follow the details of the time relaxation of the contact angle. The microscope was connected to a black-and-white CCD camera and the images (768×576 pixels—256 gray levels) of the droplet were captured with a frame grabber (Picolo Pro, Euresys, Belgium) at 50 images per second. The images are stored on a computer disk for further analysis. All the experiments were conducted at room temperature (21±1 °C). Each image was processed as follows, using the G-Contact © software. In the early stages of the relaxation process, the odd and even lines of the image are first separated from each other and the missing lines are interpolated. The reconstructed images are separated by a time laps of 40 ms. After the localization of the edge of the liquid/gas interface, the shape of sessile drops in presence of gravity was described by the Laplace equation:[21]

$$\Delta P = \gamma\left(\frac{1}{R_1}+\frac{1}{R_2}\right) \tag{4}$$

which relates the surface tension γ of the liquid to the pressure difference ΔP across the liquid/gas interface, R_1 and R_2 being the two principle radii of curvature of the curved surface. The best Laplace-curve was fitted[22] through the profile of the sessile drops (about 1500 experimental points).[11,13,20] As the axis of the camera is slightly tilted, the substrate position—and therefore the contact angles and the base radius—is determined by the cross-points between the theoretical curve fitted through the droplet profile and through its reflection on the solid substrate. In the following paragraphs, only the Tanner–Hoffman plots have been considered. The variations of the advancing contact angles and its discussion in terms of the friction coefficient ζ_0, defined by Eq. (3), will be presented elsewhere,[23] as well as the effect of the crosslinking degree of the elastomer on the contact angle relaxation process.[24]

3. Results and discussion

3.1. Characterization of the substrates

The substrates were characterized by their contact angle hysteresis and critical surface tension. The advancing and receding contact angles of MilliQ water droplets, respectively θ_a and θ_r, are 113.3 and 111.4° for the

SAM and 112.6 and 111.1° for the elastomer surface. The physical roughness is very low and does not induce the trapping of the contact line in the spreading experiments. The critical surface tension has also been measured using the homologous series of alkanes.[25,26] We obtained $\gamma_c = 20.6$ mN/m and $\gamma_c = 22.2$ mN/m for the SAM and the elastomer, respectively. These results were not influenced by the thickness of the elastomer film.

Let us first consider the impact of water droplets on the elastomer surfaces and let us compare it with the impact of droplets on the alkanethiol SAM. This comparison will help us to understand the different aspects of the energy dissipation during the impact and the spreading for surfaces with almost equivalent roughness and surface energy.

3.2. Droplet impact

The impact of Milli-Q water droplets (diameter: 2.34 mm, impact velocity: 1.73 m/s) was studied on alkanethiol self-assembled monolayers on gold substrate and on polysiloxane elastomers thick film (≃20 μm) (Fig. 4). The origin of the time (which is the impact moment) is evaluated by the impact velocity and the space between the last image before impact and the solid surface. Time between original images is 1.083 ms.

Milli-Q water was chosen as the droplet liquid because of its low viscosity and high contact angles with the chosen surfaces. In such case, the outcome of the normal impact can be varied changing the impact and surface conditions.[14,27] As for usual drop impact, the spreading phase is similar in both experiments. Most of the spreading phase is inertia dominated.[15] Despite the fact that both systems show similar static contact angles (within the 1° accuracy given by the measuring method) and that equal drop impact velocity and size are used, the receding phase is completely different in both cases. In particular cases, outcomes are very sensitive to impact and surfaces conditions[27] and the event is not so reproducible. For apparent similar impact and surface conditions such cases exhibit different outcomes from one experiment to another. The experiments provided in Fig. 4 showed a high reproducibility and no difference was visualized between repeated experiments. In the case of the elastomer, the receding phase is not energetic enough to lift up the liquid in the central jet. On the contrary for the impact on alkanethiol SAM gold surface, the drop still exhibit enough energy at the end of the receding phase to create a central jet. This jet is due to the inertia provoked by the strong receding motion. The maximum spreading diameter is 3% larger for the impact on the alkanethiol SAM gold surface than the impact on the elastomer. The main result is that, for these specific cases, the system is not well characterized by the only mention of those parameters: drop size, impact velocity, liquid surface tension and viscosity and finally wettability characterized by the static contact angles (advancing and receding). As the surfaces are smooth and the impacting processes similar and highly reproducible, the difference possibly comes from the deformation of the surface and/or the dynamic of spreading. Further investigation of the impact phenomenon on elastomer surface will be reported elsewhere.[28]

Let us now consider the spreading of silicon oil droplets as a function of the thickness of the elastomer sample—from the thinnest to the thickest—to investigate its effect on the viscoelastic breaking of the liquid.

3.3. Spreading of silicon oil droplets

Droplets of SL6600 silicon resin are spread on R-PE100 surface. The relaxation of the advancing contact angle θ towards its equilibrium value θ_0 is recorded as a function of the time. A log–log plot of $\cos\theta_0 - \cos\theta$ versus U, the speed of the contact line is drawn in Fig. 5. The data are linearly interpolated to obtain the value of the exponent characteristics of the spreading. Surprisingly, for the 3 μm thick R-PE100 sample, the value of the slope is close to 0.3, i.e. significantly different from the one expected on the basis of the viscoelastic breakdown reported by Carré and Shanahan.[4] We may therefore conclude that, in a first approximation and in this case, the viscoelastic dissipation at the level of the elastomer surface can be neglected and that only a viscous dissipation occurs in the core of the droplet.

Let us now consider the droplet spreading on the glass supported elastomer films, keeping in mind that the thickness of the elastomer layer is varied from 6.0 to 24.3 μm (Table 1).

Fig. 6a and b shows the variations of $[\cos\theta_0 - \cos\theta]$ versus U. These results should be compared to those presented in Fig. 5 for the R-PE100 film. For both the bulk elastomers (Fig. 6a) and the thin elastomer films (Fig. 6b), there is a linear relation between these two quantities and the related slopes range are in the range 0.33 ± 0.02 (thin film on PE support) to 0.61 ± 0.02 (bulk elastomers), as shown in Fig. 7.

In Fig. 7, the value of n decreases as the thickness of the film decreases. The trends is approximatively given by a sigmoid curve on a logarithmic scale for the thickness axis. One sees that, for thick films (thickness > 30 μm) and bulk elastomers, the viscoelastic breaking dominates the dissipation of energy during the spreading process, according to the predictions of Carré and Shanahan. On the contrary, at the lowest thickness, the dissipation is dominated by the molecular rearrangements of the liquid molecules in the core of the droplet, as expected for a end-methylated silicon oil for which the friction regime is completed within the first milliseconds of the spreading process.[11]

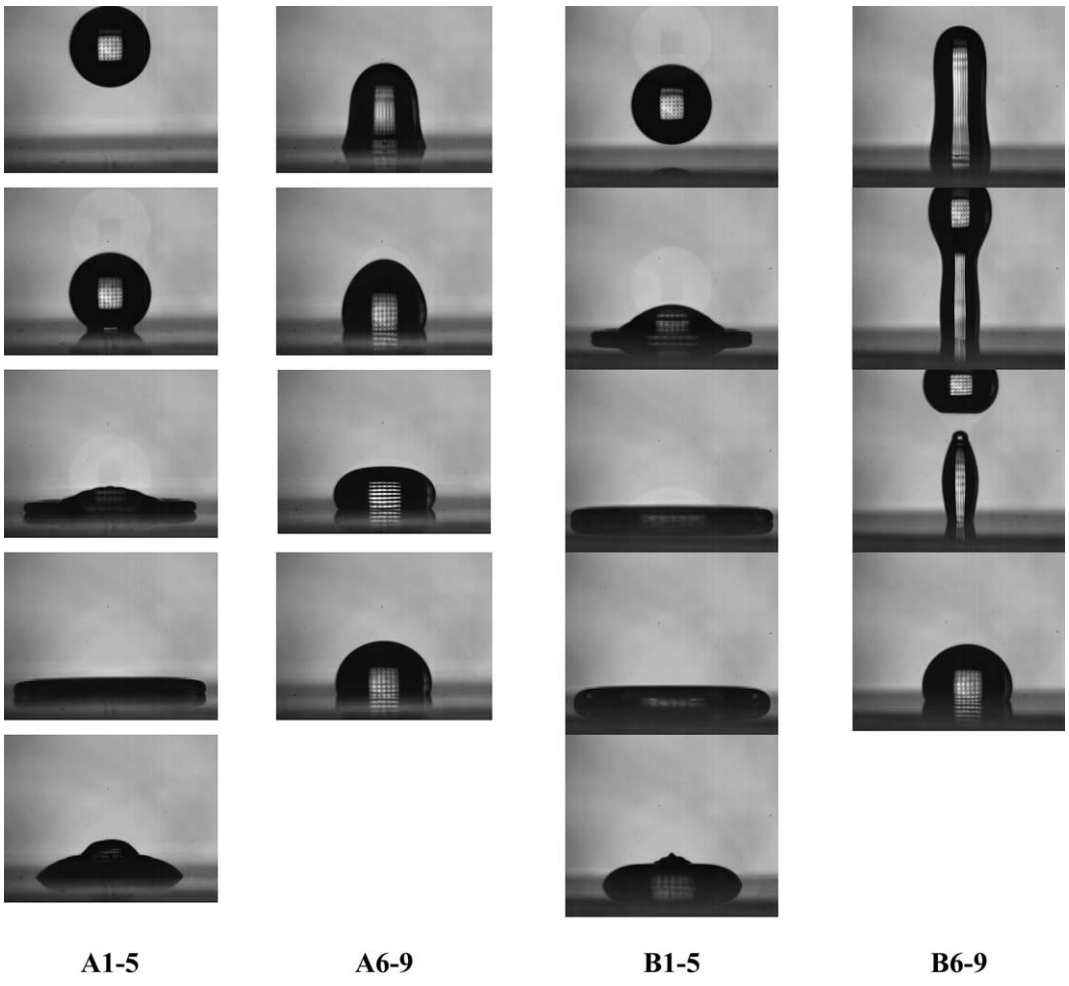

Fig. 4. Impact of water droplets (diameter: 2.34 mm). A1-9: Polysiloxane elastomer on silicon substrate (A1: before impact, A2-8: $t = 0.06$, 1.15, 2.23, 5.48, 8.73, 11.98 and 14.14 ms, A9: at equilibrium); B1-9: C_{12}-alkanethiol SAM on gold substrate (B1: before impact, B2-8: $t = 0.88$, 1.96, 3.05, 5.21, 8.46, 11.71 and 14.96 ms, B9: at equilibrium).

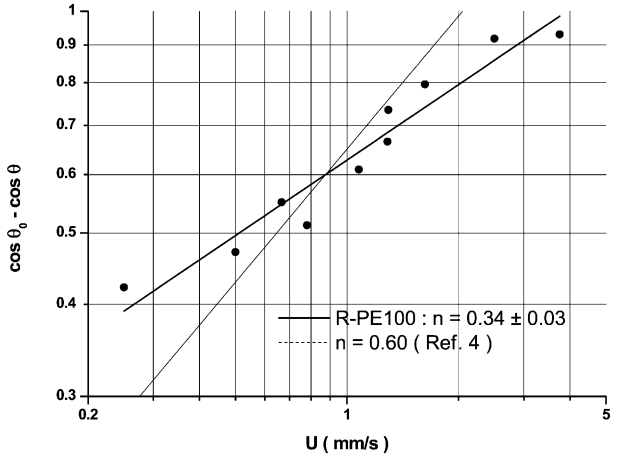

Fig. 5. Relaxation of the contact angle of a SL6600 droplet on top of a R-PE100 sample: the slope of the least-square linear fit of the experimental data (0.33 ± 0.02, plain line) does not correspond to a viscoelastic dissipation regime.[4]

3.4. Discussion

In case of the impact or of the spreading against non-deformable or "hard" solid surface, the impact energy is used in viscous dissipation in the bulk of the liquid, in creation of new liquid/air surface and work against spreading. But as the solid surface can also be soft and deformable (when the elastomer surface is 20 microns thick, or higher), part of the energy is used to deform the solid surface at the moment the liquid touches it. In this case, when the drop is reaching its maximum diameter, the energy left to retract is weaker than for the hard solid surface example. In the same way, the spreading and/or receding on such surface is slowed down[4,29] and a part of the energy is used to deform the surface during the displacement of the liquid on the solid. A logical consequence is that, as time passes, more energy is dissipated for the case of impact on the elastomer surface than on the "hard" alkanethiol SAM

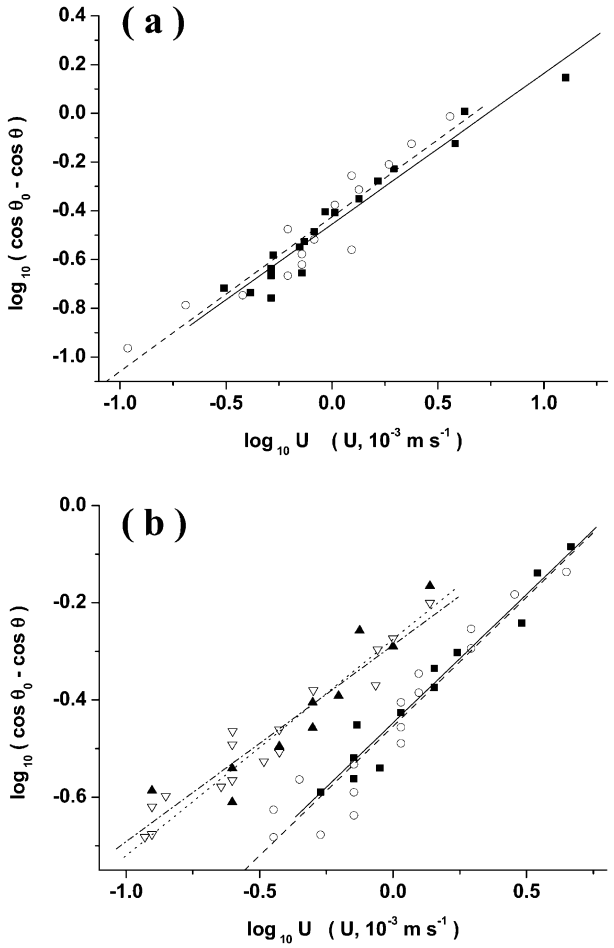

Fig. 6. Effect of elastomer thickness on the speed of the contact line. (a) bulk elastomers (Thickness: 3 mm; slope: ≃0.60) (b) elastomer films dip coated on glass (Thickness: 6.0 or 8.0 μm slopes: ≃0.40 or thickness: 12.9 or 24.1 μm; slopes: 0.50).

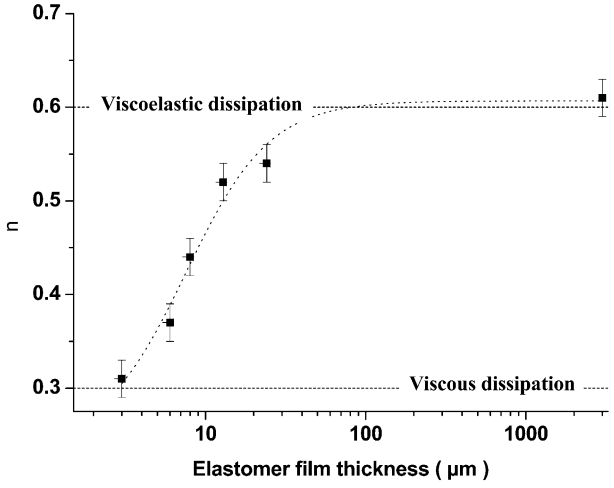

Fig. 7. Effect of elastomer thickness on the exponent n, defined by Eq. (1). The errors bars are the standard errors calculated from the covariance matrix.

gold surface. Another difference between both impact is the wettability of both systems. Even if the static contact angles are similar one can take into account the dissipation at the molecular level in the region of the contact line. This dissipation process is quantified by the measurement of the friction coefficient.[8,12] Thus difference in chemical or physical properties of the surface shall lead to difference in friction coefficient.

More precisely, to our knowledge, this is the first time that the transition for the viscoelastic regime to the viscous one is reported for an experimental system, although some theoretical investigations by Leibler and coworkers[30] pointed out that the incompressibility of the film and its finite thickness play an important role when considering the respective contributions to the deformation free energy of the elastic and of the surface tension term.

A detailed analysis of the contact angle time relaxation curves is reported elsewhere.[23] The main results are summarized hereafter. Although not explicitly corrected to take into account the deformation of the substrate, the MKT of wetting adequately reproduces the experimental data. The friction decreases as the thickness of the elastomer film increases: it goes from 13.5 mPa s at 6 μm to 9.5 mPa s at 24 μm. It should be kept in mind that this friction coefficient is not corrected for the viscoelastic behavior of the film and has therefore to be considered as an effective friction. Nevertheless, the method is highly sensitive to the thickness of the elastomer film.

4. Conclusions

We have described the impact and the spreading of liquid droplets on soft surfaces. We have shown that the impact of a water droplet on such surfaces is completely different from the one on alkanethiol SAM. The differences can be attributed to the deformation of the substrate and to the dissipation which is associated to it. In the second part of the article, we have shown that the viscoelastic breaking of the contact line of a liquid droplet spreading on the elastomer surface was a phenomenon which is thickness-dependent. Furthermore, by changing the thickness of the elastomer film, it was possible to monitor a transition between a regime of energy dissipation controlled by the viscosity of the fluid (as measured on thin films) and a regime controlled by the viscoelastic dissipation (as measured on bulk elastomers and thick films).

Acknowledgements

This work is partially supported by the Ministère de la Région Wallonne, the Belgian Funds for Scientific Research (FNRS) and the European Community.

References

1. Saiz, E., Cannon, R. and Tomsia, A., Reactive spreading: adsorption, ridging and compound formation. *Acta Mat*., 2000, **48**, 4449–4462.
2. Saiz, E., Cannon, R. and Tomsia, A., Reactive spreading in ceramic/metal systems. *Oil Gas Sci. Tech.- Rev. IFP*, 2001, **56**, 89–96.
3. Shanahan, M., Dynamique d'étalement sur solides déformables. *C.R. Acad. Sci. Paris*, 1987, **305**, 1149–1152.
4. Carré, A. and Shanahan, M., Freinage viscoélastique de l'étalement d'une goutte, C. *R. Acad. Sci. Paris*, 1993, **317**, 1153–1158.
5. Shanahan, M. and Carré, A., Anomalous spreading of liquid drops on an elastomeric surface. *Langmuir*, 1994, **10**, 1647–1649.
6. Shanahan, M. and Carré, A., Viscoelastic dissipation in wetting and adhesion phenomen. *Langmuir*, 1995, **11**, 1396–1402.
7. Carré, A. and Shanahan, M., Direct evidence for viscosity-independent spreading on soft solid. *Langmuir*, 1995, **11**, 24–26.
8. De Ruijter, M., De Coninck, J. and Oshanin, G., Droplet spreading: partial wetting regime revisited. *Langmuir*, 1999, **15**, 2209–2216.
9. Blake, T. and Haynes, J., Kinetics of liquid/liquid displacement. *J. Colloid. Int. Sci*., 1969, **30**, 421–423.
10. Blake, T., Dynamic contact angle and wetting kinetics. In *Wettability*, ed. J. Berg. Marcel Dekker, New-York, 1993, pp. 252–309.
11. De Ruijter, M., Charlot, M., Voué, M. and De Coninck, J., Experimental evidence of several times scales in drop spreading. *Langmuir*, 2000, **16**, 2363–2368.
12. De Ruijter, M., Blake, T. and De Coninck, J., Dynamic wetting studied by molecular modeling simulations of droplet spreading. *Langmuir*, 1999, **15**, 7836–7847.
13. Semal, S., Bauthier, C., Voué, M., Vanden Eynde, J., Gouttebaron, R. and De Coninck, J., Spontaeous spreading of liquid droplets on mixed alkanethiol monolayers: dynamics of wetting and wetting transition. *J. Chem. Phys. B*, 2000, **104**, 6225–6232.
14. Rioboo, R., Marengo, M. and Tropea, C., Outcomes from drop impacts onto solid surfaces. *Atomization and Sprays*, 2001, **11**, 155–166.
15. Rioboo, R., Marengo, M. and Tropea, C., Time evolution of liquid drop impact onto solid, dry surfaces. *Exp. Fluids*, 2002, **33**, 112–124.
16. Roisman, I., Rioboo, R. and Tropea, C., Normal impact of liquid drop on Dry surface: model for spreading and receding. *Proc. R. Soc. London*, 2002, **458**, 1411–1430.
17. Mourougou-Candoni, N., Prunet-Foch, B., Legay, F., Vignes-Adler, M. and Wong, K., Influence of dynamic surface tension on the spreading of surfactant solution droplets impacting onto low-surface-energy solid substrate. *J. Colloid Int. Sci*., 1997, **192**, 129–141.
18. Chandra, S. and Avedisian, C., On the collision of droplet with solid surface. *Proc. R. Soc. London*, 1991, **432**, 13–41.
19. Richard, D. and Quéré, D., Bouncing water drops. *Europhys. Lett*., 2000, **50**, 769–775.
20. Semal, S., Voué, M., Dehuit, J., de Ruijter, M. and De Coninck, J., Dynamics of spontaneous spreading on heterogeneous surfaces in the partial wetting regime. *J. Phys. Chem. B*, 1999, **103**, 4854–4861.
21. Rusanov, A. and Prokhorov, V., *Interfacial Tensiometry*. Elsevier, Amsterdam, 1996.
22. Press, W., Teutlosky, S., Vetterling, W. and Flannery, B., *Numerical Recipes in FORTRAN. The Art of Scientific Computing*. Cambridge University Press, Cambridge, 1992.
23. Charlot, M., Voué, M. and De Coninck, J. Wettability, frictional and adhesive properties of polysiloxane elastomers. *Langmuir* (submitted for publication).
24. Voué, M., Charlot, M. and De Coninck, J. Crosslinking degree of polysiloxane elastomer thin films from wettability experiments. *Int. J. Adhes. Adhes.* (submitted for publication).
25. Good, R. and Girifalco, L., A theory for estimation of surface and interfacial energies. III. Estimation of surface energies of solids from contact angle data. *J. Phys. Chem*., 1960, **64**, 561–565.
26. Zisman, W., Relation of the equilibrium contact angle to liquid and solid constitution. *Adv. Chem. Ser*., 1964, **43**, 1–51.
27. Rioboo, R., *Impact de Gouttes Sur Surfaces Solides et Sèches*. PhD thesis, Université Pierre et Marie Curie, Paris, 2001.
28. Rioboo, R., Voué, M., Bauthier, C., Conti, J. and De Coninck, J., Impact of droplet on soft surfaces: beyond the static contact angle. *Langmuir* (submitted for publication).
29. Tomasetti, E., Rouxhet, P. and Legras, R., Viscoelastic behavior of polymer surface during wetting and dewetting processes. *Langmuir*, 1998, **14**, 3435–3439.
30. Long, D., Ajdari, A. and Leibler, L., Static and dynamic wetting properties of thin rubber films. *Langmuir*, 1996, **12**, 5221–5230.